JACS
JOURNAL OF THE AMERICAN CHEMICAL SOCIETY

Article

pubs.acs.org/JACS

Competition of Charge- versus Radical-Directed Fragmentation of Gas-Phase Protonated Cysteine Sulfinyl Radicals

Chasity B. Love, Lei Tan, Joseph S. Francisco,* and Yu Xia*

Department of Chemistry, Purdue University, West Lafayette, Indiana 47907-2084, United States

Supporting Information

ABSTRACT: The fragmentation behavior of various cysteine sulfinyl ions (intact, N-acetylated, and O-methylated), new members of the gas-phase amino acid radical ion family, was investigated by low-energy collision-induced dissociation (CID). The dominant fragmentation channel for the protonated cysteine sulfinyl radicals ($^{SO\bullet}$Cys) was the radical-directed $C_\alpha-C_\beta$ homolytic cleavage, resulting in the formation of glycyl radical ions and loss of CH_2SO. This channel, however, was not observed for protonated N-acetylated cysteine sulfinyl radicals (Ac-$^{SO\bullet}$Cys); instead, charge-directed H_2O loss followed immediately by SH loss prevailed. Counterintuitively, the H_2O loss did not derive from the carboxyl group but involved the sulfinyl oxygen, a proton, and a C_β hydrogen atom. Theoretical calculations suggested that N-acetylation significantly increases the barrier (~14 kcal mol^{-1}) for the radical-directed fragmentation channel because of its reduced capability to stabilize the thus-formed glycyl radical ions via the captodative effect. N-Acetylation also assists in moving the proton to the sulfinyl site, which reduces the barrier for H_2O loss. Our studies demonstrate that for cysteine sulfinyl radical ions, the stability of the product ions (glycyl radical ions) and the location of the charge (proton) can significantly modulate the competition between radical- and charge-directed fragmentation.

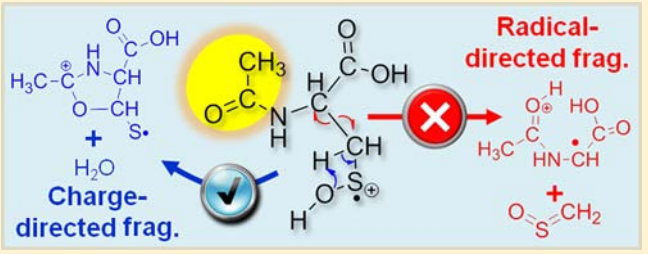

INTRODUCTION

Protein radicals play important roles in biological systems, including their involvement in enzyme catalytic sites,[1] inflammatory response,[2,3] and oxidative damage of proteins.[4,5] The chemical properties of protein radicals are intriguing but have not been extensively explored because of the difficulty of probing these transient species in solution. Studies of the analogues of protein radicals, such as amino acid radical ions in the gas phase, allow an alternative way of interrogating the intrinsic chemistry of protein radicals. A variety of mass spectrometric approaches have been used to investigate radical ions of amino acids,[6−8] simple peptides,[9−13] and even proteins[14,15] based on collision-induced dissociation (CID), ion/molecule reactions,[16,17] and ion spectroscopy.[18,19] These experimental results together with insight from theoretical calculations provide useful information on radical ions' structure, energetics, and reactivity.

Because of the coexistence of the radical and charge, the gas-phase ion chemistry of radical ions can be drastically different from that of their even-electron counterparts[20] The various combinations of the radical location and the charge location give rise to a large number of structural isomers. For instance, the structure of an amino acid radical ion can be either "canonical", where the charge and spin are located at the same place (typically on the side chain of an amino acid residue); "captodative",[21] where the radical is at the α-carbon and the charge is on the carbonyl oxygen; or "distonic,[22−24] where the charge and radical site reside and function independently. The change from one isomeric structure to another may involve intramolecular transfers of both protons and hydrogen atoms.[25,26] The highest energy barriers for the above processes determine the stability of each structural isomers. Among the few amino acid radical cations that have been both experimentally and theoretically studied, the captodative structures are found to be energetically favorable in most cases (e.g., glycine,[6] histidine,[27] cysteine,[8,18] arginine,[28] tyrosine[29]), while a few prefer a canonical structure upon formation.[30] The structural diversity also presents fascinating chemistry in which a larger dimension of tuning is made available by the coexistence of the radical site and charge in comparison with even-electron ions. This aspect has aroused considerable fundamental interest in probing the roles of the radical and the charge in affecting the chemistry of the ion upon excitation or reaction. Recent studies of hydrogen-deficient peptide radical ions (i.e., those having fewer hydrogen atoms than the intact peptide ions) showed a competition between radical- and charge-directed fragmentation. The radical-directed fragmentation channels included both side-chain losses and peptide backbone fragmentation ($N-C_\alpha$ and $C_\alpha-C_\beta$ cleavages),[25,31−34] while amide bond cleavage was mainly observed from charge-directed fragmentation.[35] The competition was found to be sensitive to the ion charge state and polarity,[36−38] the amino acid composition,[39−41] the ease of mobilizing a proton versus a radical,[42] and the relative barriers for radical isomer-

Received: January 25, 2013
Published: March 25, 2013

   dx.doi.org/10.1021/ja4008744 | J. Am. Chem. Soc. 2013, 135, 6226−6233

ization versus fragmentation.[43−45] Factors affecting the competition within amino acid radical ions have not been systematically explored.

Cysteine sulfinyl radical ($^{SO\bullet}$Cys) is a new member of the gas-phase amino acid radical family whose formation was recently reported by our group.[37,38,46] The existence of cysteine sulfinyl radicals within proteins or peptides, however, was previously detected in solution by electron paramagnetic resonance spectroscopy when an anaerobic enzyme utilizing glycyl radicals for catalysis was exposed to air or small disulfide peptides were under radical attack.[47−49] It was postulated that the sulfinyl radical (R−SO$^{\bullet}$) is an intermediate that forms upon oxidation of thiyl radical and that it might participate in adjusting the glycyl/thiyl radical equilibrium. The intrinsic chemical properties of cysteine sulfinyl radicals have not been systematically studied. A recent paper by our group surveyed the CID behavior of a series of site-specific peptide sulfinyl radical ions.[37] A unique radical-driven fragmentation channel, namely, the loss of CH_2SO (62 Da), was identified, likely from C_α−C_β bond scission on the cysteine sulfinyl radical side chain. Its competition with other charge-driven fragmentation processes, such as proton-catalyzed peptide amide bond dissociation, was found to be enhanced for peptide systems lacking mobile protons.

In this study, we used simple cysteine sulfinyl radical ions ([$^{SO\bullet}$Cys + H]$^+$) and their derivatives as model systems to investigate further the structures of these radical ions, the fragmentation mechanisms and energetics of the radical-driven CH_2SO loss, and the key factors affecting the competition of this channel with other charge-driven processes under low-energy CID conditions. Accurate mass measurements, tandem mass spectrometry (MS^n), and stable isotopic labeling were employed to provide experimental evidence that was further correlated and explained using theoretical calculations.

EXPERIMENTAL SECTION

Materials. L-Cystine, *N*-acetyl-L-cysteine, *N*-acetyl-L-cysteine methyl ester, and L-cysteine-2,3,3-d_3 were purchased from Sigma-Aldrich (St. Louis, MO). L-Cysteine methyl ester hydrochloride was purchased from Tokyo Chemical Industry Co., Ltd. (Tokyo, Japan). DL-Cysteine-3,3-d_2 was purchased from Cambridge Isotope Laboratories, Inc. (Andover, MA). *N*-Acetyl-L-cysteine-3,3-d_2 and *N*-acetyl-L-cysteine-2,3,3-d_3 were synthesized in house. Acetylation was achieved by mixing the amino acid solution (50 μL of 50 mM ammonium bicarbonate/50 μL of 1 mg/mL cystine) with 50 μL of acetylation reagent (20 μL of acetic anhydride and 60 μL of methanol). Disulfide bond formation within derivatized cystine was performed by dissolving cysteine derivatives in water (1 mg/mL) and allowing air oxidation for 2−4 days. ^{18}O labeling was achieved by dissolving 1 mg of *N*-acetyl-L-cysteine in 100 μL of $H_2{}^{18}O$ for 3−7 days at room temperature. The solution was further diluted to 0.1 mg/mL with methanol. For solution H/D exchange experiments, 1 mg/mL solutions of cystine derivatives were diluted 100-fold in 50:50 acetonitrile/D_2O containing 1% acetic acid. The degree of reaction was monitored by mass spectrometric analysis. Working solutions for positive nanoelectrospray ionization (nanoESI) were prepared at 10 μM in 50:49:1 (v/v/v) MeOH/H_2O/HOAc.

Mass Spectrometry. Unless otherwise specified, all experiments were performed on a 4000 QTRAP tandem mass spectrometer having a triple quadrupole/linear ion trap configuration (AB SCIEX, Toronto, Canada). For ion trap CID, precursor ions were isolated in the Q1 quadrupole, transferred through the collision cell (Q2) with minimum kinetic energy, and again isolated in the Q3 linear ion trap, and the collisional activation was conducted using dipolar excitation. Instrument control, data acquisition, and processing were carried out using Analyst 1.5 software. The typical parameters for the 4000 QTRAP instrument were set as follows: spray voltage, 1400−1800 V; collision energy, 10−25 V; ion trap activation amplitude, 10−20 mV; curtain gas, 10−15 psi; declustering potential, 20−30 V; scan rate, 1000 Da/s. The data reported here are averages of typically 50 scans. Accurate mass measurements were obtained on an LTQ-Orbitrap instrument (Thermo Fisher Scientific, San Jose, CA) with a resolution of 30 000 and the use of internal mass calibration. Intact and modified cysteine sulfinyl radical ions were formed from atmospheric-pressure ion/radical reactions, which occurred when the nanoESI plume of intact or modified cystine was allowed to interact with oxidative radicals (OH or others) in the afterglow region of an atmospheric pressure (AP) helium low-temperature plasma (LTP).[37]

COMPUTATIONAL DETAILS

All of the calculations were performed using Gaussian 09.[50] Three levels of theory were used in preliminary searches for global minima and transition states: restricted and unrestricted Hartree−Fock (RHF and UHF, respectively), unrestricted second-order Møller−Plesset perturbation theory (MP2), and density functional theory using the Becke nonlocal three-parameter exchange/Lee−Yang−Parr correlation hybrid functional (B3LYP).[51,52] Geometry optimizations were carried out for all structures using Schlegel's method to better than 0.001 Å for bond lengths and 0.01° for angles, with a self-consistent field convergence of at least 10^{-9} on the density matrix. The residual root-mean-square (rms) force was less than 10^{-4} a.u. Once an optimized structure was found, vibrational frequency calculations were performed to verify whether the structure was a minimum (all frequencies real) or a first-order saddle point (one imaginary frequency). The 6-31G(d) basis set was used in the calculations. The proper connectivity between reactants, prereactive complexes, transition states, and products was verified by intrinsic reaction coordinate (IRC) calculations.[53] The B3LYP method is a widely used for studying the structure, reactivity, and dissociation of amino acid and peptide radical cations. Single-point energies were calculated using the coupled-cluster single and double excitation with perturbation estimate of the triple excitation [CCSD(T)] method[54] in order to incorporate electron correlation. All of the calculations were corrected with vibrational zero-point energy (ZPE). CCSD(T)//B3LYP/6-31G(d)+ΔZPE was the level of theory used to obtain the relative enthalpies reported later in the text. Moreover, for open-shell systems, the value of $\langle S^2 \rangle$ did not show major deviations from 0.75.

RESULTS

Formation of Gas-Phase Intact Cysteine and Modified Cysteine Sulfinyl Radical Ions. Our group previously developed a method to form site-specific peptide sulfinyl radical ions in which interchain disulfide-linked peptide ions entrained in the nanoESI plume are allowed to react with oxidative radicals (i.e., OH) produced from an AP helium LTP right before entering the mass spectrometer.[37] Upon cleavage of the disulfide bond, R−SOH/R−S$^{\bullet}$ and R−SO$^{\bullet}$/R−SH pairs are formed as the major reaction products at the cleavage site. The same method and setup was used to form the cysteine and derivatized cysteine sulfinyl radical ions studied herein. Relatively pure sulfinyl radical ions with adequate intensities were generally observed. Figure S1 in the Supporting Information shows typical AP ion/radical reaction mass spectra of L-cystine and *N*-acetyl-L-cystine in positive ionization mode. The superscript "SO•" is used to indicate the formation of sulfinyl radicals in later discussions.

Unimolecular Dissociation of Cysteine and Derivatized Cysteine Sulfinyl Radical Ions. Unimolecular dissociation of protonated L-cysteine sulfinyl radical ($^{SO\bullet}$Cys) and its three derivatives, *N*-acetyl-L-cysteine sulfinyl radical (Ac-$^{SO\bullet}$Cys), L-cysteine methyl ester sulfinyl radical ($^{SO\bullet}$Cys-OMe), and *N*-acetyl-L-cysteine methyl ester sulfinyl radical (Ac-$^{SO\bullet}$Cys-OMe) was investigated by ion trap collisional activation. Figure 1 shows MS^2 CID mass spectra of protonated $^{SO\bullet}$Cys and Ac-$^{SO\bullet}$Cys, while the data for $^{SO\bullet}$Cys-OMe and Ac-$^{SO\bullet}$Cys-OMe are shown

dx.doi.org/10.1021/ja4008744 | J. Am. Chem. Soc. 2013, 135, 6226−6233

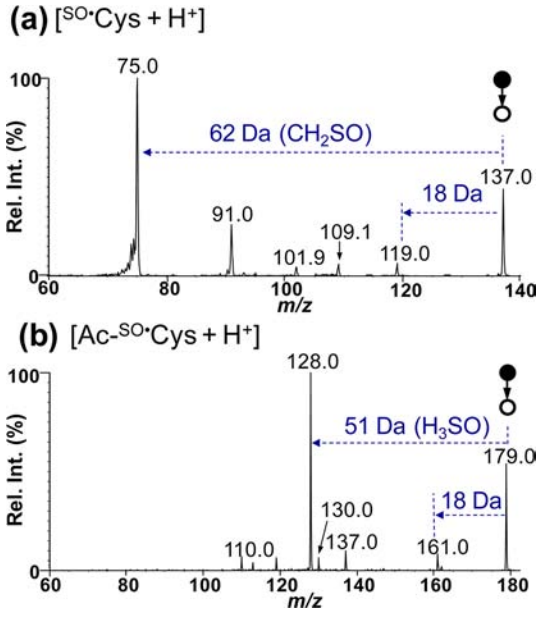

Figure 1. MS^2 CID of protonated (a) ^{SO}•Cys and (b) Ac-^{SO}•Cys.

in Figure S2 in the Supporting Information. Collisional activation of protonated ^{SO}•Cys (m/z 137) resulted in the loss of a 62 Da fragment (i.e., a peak at m/z 75) as the major fragmentation channel (Figure 1a). This loss, likely a cleavage from the cysteinyl side chain, was observed previously from CID of peptide sulfinyl ion systems and identified as CH_2SO loss on the basis of accurate mass measurements.[37,38] We further confirmed this loss by conducting MS^2 CID on L-cysteine-3,3-d_2 sulfinyl radical ions (d_2-^{SO}•Cys), in which the two C_β hydrogens are labeled with deuterium (Figure S3 in the Supporting Information). The observed major fragmentation channel shifted to a 64 Da loss, indicating the incorporation of the two deuteriums. This observation confirmed that the lost 62 Da fragment (CH_2SO) was indeed formed from the cysteine sulfinyl radical side chain. A possible fragmentation pathway leading to CH_2SO loss via C_α–C_β homolytic cleavage is shown in Scheme 1 below. Besides this main fragmentation channel, other minor fragments included the losses of 18 Da (m/z 119), 28 Da (m/z 109), 35 Da (m/z 102, corresponding to consecutive H_2O and NH_3 losses), and 46 Da (m/z 91).

The fragmentation pattern from MS^2 CID of protonated Ac-^{SO}•Cys (m/z 179) (Figure 1b) was drastically different from that of ^{SO}•Cys (Figure 1a). The 62 Da loss (m/z 112) was not observed above the noise level; instead, the loss of 51 Da (m/z 128) became the dominant fragmentation channel. Accurate mass measurement provided a mass of 50.9904 Da, corresponding to an elemental composition of H_3SO (theoretical mass 50.9905 Da). In view of the complicated rearrangements needed to obtain H_3SO loss, it is unlikely that this fragmentation happened in a single step. In order to unveil the 51 Da loss, CID was conducted on protonated *N*-acetyl-3,3-d_2 sulfinyl radicals (d_2-Ac-^{SO}•Cys, m/z 181), in which the two C_β hydrogen atoms in the cysteine side chain are replaced by deuterium. The MS^2 CID data for d_2-Ac-^{SO}•Cys are shown in Figure 2a. The dominant fragmentation channel was the loss of 52 Da (m/z 129). Upon comparison with the 51 Da loss from the nonlabeled species (Figure 1b), this observation established that one of the C_β hydrogen atoms was involved. Interestingly, a 19 Da loss (m/z 162) was also present, indicating the involvement of one C_β hydrogen in the water loss (HDO) as well. Figure 2b shows MS^3 CID of the 19 Da loss obtained from Figure 2a. A dominant 33 Da loss (SH) was observed at m/z 129. The data in Figure 2a,b unambiguously demonstrate that the 51 Da loss (H_3SO) from CID of Ac-^{SO}•Cys indeed resulted from sequential fragmentation (i.e., H_2O loss followed by SH loss). Moreover, the C_β hydrogen was involved only in the H_2O loss step but not in the SH loss step. It should be noted that MS^2 CID of protonated d_2-^{SO}•Cys (C_β labeled with two deuteriums; Figure S3 in the Supporting Information) showed only the loss of 18 Da without any loss of 19 Da (HDO), signifying that the H_2O loss from ^{SO}•Cys results from another channel. In addition, MS^3 CID of H_2O loss from ^{SO}•Cys did not result in SH loss. The major fragmentation

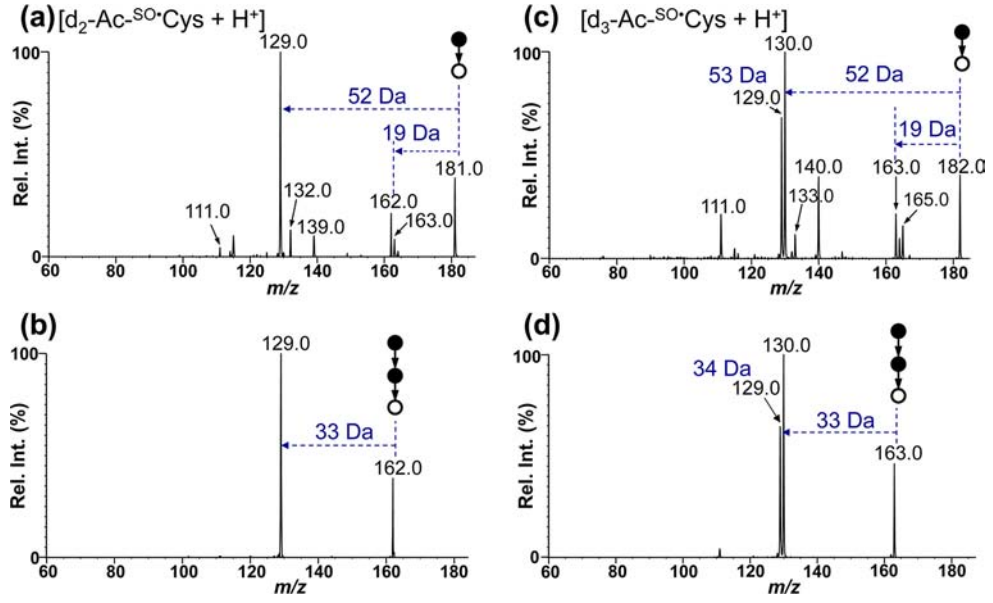

Figure 2. MS^2 CID of protonated (a) d_2-Ac-^{SO}•Cys and (c) d_3-Ac-^{SO}•Cys. MS^3 CID of the 19 Da losses (HDO) in (a) and (c) are shown in (b) and (d), respectively.

dx.doi.org/10.1021/ja4008744 | J. Am. Chem. Soc. 2013, 135, 6226–6233

Scheme 1. Possible Reaction Pathway for CH_2SO Loss from Protonated $^{SO\bullet}$Cys Radicals

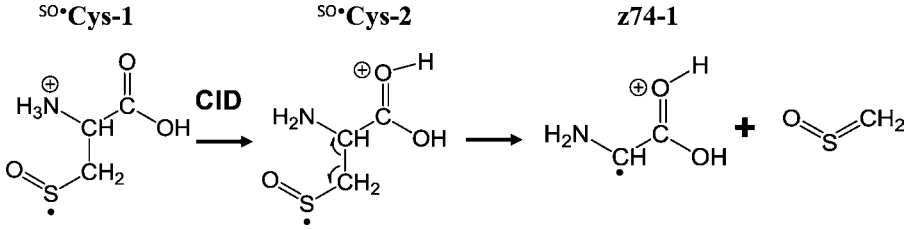

channel was sequential loss of H_2O (Figure S4 in the Supporting Information).

We further studied CID of protonated *N*-acetyl-2,3,3-d_3 sulfinyl radicals (d_3-Ac-$^{SO\bullet}$Cys, m/z 182), in which all of the C_α and C_β hydrogens were replaced by deuterium. As shown in Figure 2c, losses of 52 Da (H_2DSO) and 53 Da (HD_2SO) were both observed, with the former having a slightly higher intensity. Loss of 19 Da (HDO) was also present, while the absence of a loss of 20 Da (D_2O) suggests that the C_α hydrogen is not involved in the water loss step. MS^3 CID of the 19 Da loss (m/z 163) is shown in Figure 2d. Both the 33 Da loss (m/z 130) and 34 Da loss (m/z 129) were present with an intensity ratio similar to that in Figure 2c. The above results again corroborate the hypothesis that H_3SO loss is formed from sequential H_2O and SH loss. In addition, two pathways are involved in the SH loss step. That is, the hydrogen can come either from C_α (34 Da loss) or from a nonlabeled position (33 Da loss), which could be either a mobile proton or the acetyl hydrogen ($-CH_3$ group). We further performed CID on d_5-Ac-$^{SO\bullet}$Cys (m/z 184; Figure S5 in the Supporting Information), in which the three exchangeable hydrogens (two hydrogens attached to oxygens and one amide hydrogen) and the two C_β hydrogens were replaced by deuterium. Loss of 20 Da (D_2O) was clearly detected, suggesting that a mobile proton is involved in the H_2O loss step. Moreover, the observation of a loss of 54 Da (D_3SO, m/z 130) in Figure S5 proves that a mobile proton is also involved in the SH loss step.

^{18}O labeling was used to investigate the origin of oxygen in the H_2O loss step. MS^2 CID was conducted on acetylcysteine sulfinyl radical ions, in which the two oxygens in the carboxyl group were ^{18}O-labeled ($^{18}O_2$-Ac-$^{SO\bullet}$Cys, m/z 183; Figure S6a in the Supporting Information). The major fragments included losses of 51 Da (H_3SO, m/z 132) and 18 Da (H_2O, m/z 165). MS^3 CID of the peak corresponding to H_2O water loss (Figure S6b in the Supporting Information) consistently produced SH loss as the major product. We noticed that there were also minor losses of 20 Da ($H_2{}^{18}O$) and 53 Da ($H_3S^{18}O$). These losses should come from a small fraction of parent ions that were ^{18}O-labeled at the sulfinyl group, which were likely formed from reactions with ^{18}OH. These results therefore suggest that the sulfinyl radical side chain is involved H_2O loss.

Ion trap CID was applied to protonated cysteine methyl ester sulfinyl radicals ($^{SO\bullet}$Cys-OMe, m/z 151) and *N*-acetyl-*O*-methyl sulfinyl radicals (Ac-$^{SO\bullet}$Cys-OMe, m/z 193) to investigate the possible role of the carboxyl group. It turned out that O-methylation did not play significant role in affecting the losses of 62 and 51 Da. The 62 Da loss was still the dominant channel in MS^2 CID of $^{SO\bullet}$Cys-OMe ions (Figure S2 in the Supporting Information), similar to that of the $^{SO\bullet}$Cys ions, while the 51 Da loss was the most abundant peak in CID of Ac-$^{SO\bullet}$Cys-OMe.

DISCUSSION

CH_2SO Loss. CH_2SO loss was the most abundant fragmentation channel from protonated $^{SO\bullet}$Cys, while it was not observed from protonated Ac-$^{SO\bullet}$Cys radicals. The experimental results showed that this loss should result from $C_\alpha-C_\beta$ bond scission, forming protonated glycyl radical ions and CH_2SO. CCSD(T)//B3LYP/6-31G(d) calculations were utilized to provide insight into the structures and energetics of protonated $^{SO\bullet}$Cys ions. We found four relatively stable structures. The most stable structure for $^{SO\bullet}$Cys is distonic (**$^{SO\bullet}$Cys-1**), in which the charge is located on the amine group and the spin is delocalized almost equally between sulfur and oxygen within the sulfinyl group. Protonation of the sulfinyl group gives rise to a canonical structure (**$^{SO\bullet}$Cys-3**) with both the charge and the radical localized on the sulfur atom. This tautomer is 14.8 kcal mol^{-1} higher in enthalpy relative to **$^{SO\bullet}$Cys-1**. With protonation at the carboxyl group, the radical can reside either on the sulfur atom in the sulfinyl group (**$^{SO\bullet}$Cys-2**) or on C_α of the cysteine, the latter of which has a captodative structure (**$^{SO\bullet}$Cys-4**). These two structures are 18.2 kcal mol^{-1} and 14.1 kcal mol^{-1} higher in enthalpy than **$^{SO\bullet}$Cys-1**, respectively. The populations of these four structural isomers upon the formation of $^{SO\bullet}$Cys radicals at room temperature was unclear. Theoretical studies showed that structures **$^{SO\bullet}$Cys-3** and **$^{SO\bullet}$Cys-4** are not directly involved in the 62 Da loss. If the most stable structure, **$^{SO\bullet}$Cys-1**, is involved in the 62 Da loss, the amine proton must migrate to the carbonyl oxygen (**$^{SO\bullet}$Cys-2**), which is followed by $C_\alpha-C_\beta$ bond scission. The overall reaction is endothermic by 42.6 kcal mol^{-1}, which should be within the attainable range of ion trap CID. It should be noted that the thus-formed glycyl radical ions (**z74-1**), which have a captodative structure with the spin located at C_α and the proton attached to the carbonyl oxygen, are 12.8 kcal mol^{-1} more stable in enthalpy than the structures with the proton attached to the amine. This result is consistent with reports from other groups on the most stable structure of glycyl radical cations.[6,7] The proposed fragmentation pathway is summarized in Scheme 1, and the potential energy surface for the corresponding process is shown in Figure 3a. The relative enthalpies for the key ion structures involved in the 62 Da loss are summarized in Table S1 in the Supporting Information, while the corresponding spin densities and charge locations are shown in Table S2 in the Supporting Information.

H_2O Loss. H_2O loss was shown to be the first step leading to H_3SO loss in acetylated cysteine sulfinyl radical ions. The most stable structure for protonated Ac-$^{SO\bullet}$Cys has the charge localized on the acetyl carbonyl group and the radical delocalized between sulfur and oxygen in the sulfinyl group (**Ac-$^{SO\bullet}$Cys-1**). This structure is 6.6, 8.0, and 10.8 kcal mol^{-1} lower in enthalpy than the structures obtained by protonation at the carboxylic site (**Ac-$^{SO\bullet}$Cys-3**), the acetyl nitrogen site (**Ac-$^{SO\bullet}$Cys-4**), and the sulfinyl radical site (**Ac-$^{SO\bullet}$Cys-2**), respectively. For all of the structures except that with protonation at the sulfinyl group

dx.doi.org/10.1021/ja4008744 | J. Am. Chem. Soc. 2013, 135, 6226−6233

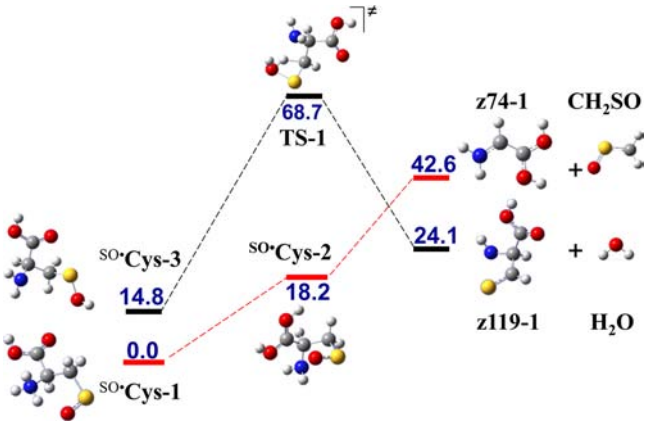

Figure 3. Energetic profile and key structures involved in the loss of (a) CH_2SO (red curve, major channel) and (b) H_2O (black curve, not observed) from protonated $^{SO•}$Cys radicals. The enthalpies are shown in kcal mol^{-1} and are relative to **$^{SO•}$Cys-1**.

(canonical structure), the radical is delocalized between the sulfur and oxygen on the cysteine side chain.

Protonation at the sulfinyl group is of special interest, since it is the most probable structure leading to H_2O loss. Stable isotopic labeling experiments suggested that both the C_β hydrogen and the sulfinyl oxygen in the protonated Ac-$^{SO•}$Cys ions are involved in the water loss step. On the basis of these observations, a possible mechanism for H_2O loss is proposed in Scheme 2, in

Scheme 2. Possible Reaction Pathway for H_2O Loss from Protonated Ac-$^{SO•}$Cys Radicals

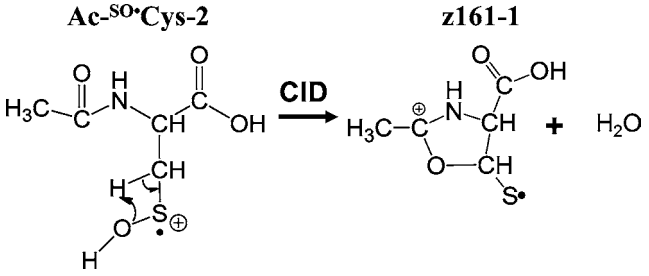

which sulfinyl-protonated Ac-$^{SO•}$Cys goes through a four-membered-ring transition state involving one C_β hydrogen, C_β, the sulfinyl oxygen, and the sulfur atom. Theoretical calculations suggested that the enthalpy of this transition state is 49.9 kcal mol^{-1} higher than that of sulfinyl-protonated Ac-$^{SO•}$Cys. After an immediate water loss, a five-membered ring (oxazoline) with the charge delocalized among the acetyl carbon and nitrogen and the radical located on sulfur (**z161-1**) is formed. The overall reaction for the water loss is exothermic by 0.5 kcal mol^{-1}. The reaction potential energy surfaces and the key structures are indicated in Figure 4b. The relative enthalpies of the key structures for H_2O loss from Ac-$^{SO•}$Cys radicals can be found in Table S1 in the Supporting Information, and the spin densities and charge locations are summarized in Table S2 in the Supporting Information.

Competition between CH_2SO Loss and H_2O Loss. One most interesting and intriguing phenomenon from CID of cysteine sulfinyl radical ions is that amine acetylation completely shuts down the radical-directed CH_2SO loss while promoting the charge-directed H_2O loss. To understand the nature of the competition between the two fragmentation channels, the potential energy surfaces for the unobserved channels (i.e., H_2O loss from protonated $^{SO•}$Cys and CH_2SO loss from protonated Ac-$^{SO•}$Cys) were also calculated and are shown in Figures 3b and 4a, respectively. As compared in Figure 3, the H_2O loss from protonated $^{SO•}$Cys goes through transition state **TS-1**, which is 26.1 kcal mol^{-1} higher than that for C_α–C_β bond scission to give CH_2SO loss (**z74-1** + **CH_2SO**). The large energy difference between the two fragmentation channels could explain the experimental observation that H_2O loss from the sulfinyl side chain with subsequent SH loss was not observed for protonated $^{SO•}$Cys. In the case of Ac-$^{SO•}$Cys (Figure 4), the barrier for H_2O loss versus C_α–C_β bond scission are different by only 4.2 kcal mol^{-1}, consequently making the two pathways energetically competitive. The dominant H_2O loss from CID of protonated Ac-$^{SO•}$Cys without CH_2SO loss suggested that the former process proceeds with much more favorable kinetics.

Acetylation of the amine might play multiple roles in enhancing charge-directed H_2O loss. First, the *N*-acetylglycyl radical ions (**z117-1**) resulting from CH_2SO loss are energetically much more costly to form, which may be a consequence of the reduced electron-donating capability of the amide compared with a free amine in stabilizing α-carbon radical cations through the captodative effect.[21] This factor should be the main reason that CH_2SO loss is not observed in the N-acetylated systems. On the other hand, N-terminal acetylation is a common method used to decrease the proton affinity of the amine by changing it to an amide.[33,35] Because of this modification, protonation at the sulfinyl group (**Ac-$^{SO•}$Cys-2**), which is a prerequisite for H_2O loss, becomes more competitive. Moreover, a five-membered-ring radical ion (**z161-1**) is formed after H_2O loss from protonated Ac-$^{SO•}$Cys. This relatively stable structure may also contribute to lowering the transition state for H_2O loss by ~4 kcal mol^{-1}. As discussed below, **z161-1** is energetically favorable for a sequential SH loss, which can further drive H_2O loss.

Sequential SH Loss. The MS^3 CID data for protonated d_3-Ac-$^{SO•}$Cys (Figure 2d) clearly suggest that there are two competing pathways leading to consecutive SH loss. One pathway possibly involves the mobile proton and the other one is associated with the C_α hydrogen. Scheme 3a shows a two-step proton transfer process that involves movement of the proton from the nitrogen site (**z161-1**) to the carbonyl oxygen (**z161-2**) through transition state **TS-3**. The proton transfer can occur from either of the OH groups; however, one group requires a C–C bond rotation of the carboxyl group (**TS-4**) and proton transfer from the carboxyl oxygen to the sulfur radical (**z161-3**). Once the sulfur is protonated, there is a subsequent loss of SH, resulting in a five-membered-ring structure (**z128-2**) with the charge localized on the β-carbon. The corresponding potential energy surfaces and key structures are shown in Figure 5a. The overall reaction is endothermic by 48.2 kcal mol^{-1}. An alternative mobile proton pathway can be initiated by a one-step proton transfer directly from the amine nitrogen (**z161-1**) to the sulfur atom via a five-membered-ring transition state followed by immediate SH loss to form **z128-2**. The two fused five-membered rings contained in the transition state (potential energy surface profile in Figure S7) effectively elevate the transition state of this strained structure (**TS-6**) to 56.7 kcal mol^{-1} relative to **z161-1**, which is significantly higher than that of the two-step proton transfer process. Therefore, the two-step proton transfer process is likely to be the main pathway even when both transition states can be reached. We also tested a pathway for SH loss starting from structure **z161-2** that involves simultaneous transfer of the carbonyl proton to sulfur and the C_α

dx.doi.org/10.1021/ja4008744 | J. Am. Chem. Soc. 2013, 135, 6226–6233

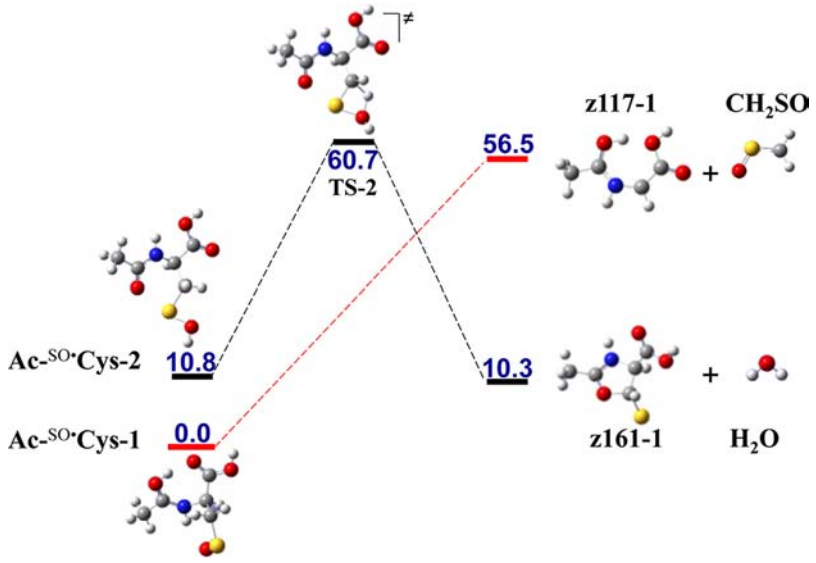

Figure 4. Energetic profile and key structures involved in the loss of (a) CH_2SO (red curve, not observed) and (b) H_2O (black curve, major channel) from protonated Ac-$^{SO•}$Cys radicals. The enthalpies are shown in kcal mol^{-1} and are relative to **Ac-$^{SO•}$Cys-1**.

Scheme 3. Possible Reaction Pathways for Consecutive SH Loss after H_2O Loss from Protonated Ac-$^{SO•}$Cys Radicals: (a) Charge-Directed Two-Step Proton Transfer Process; (b) Radical-Directed SH Loss Involving the C_α Hydrogen

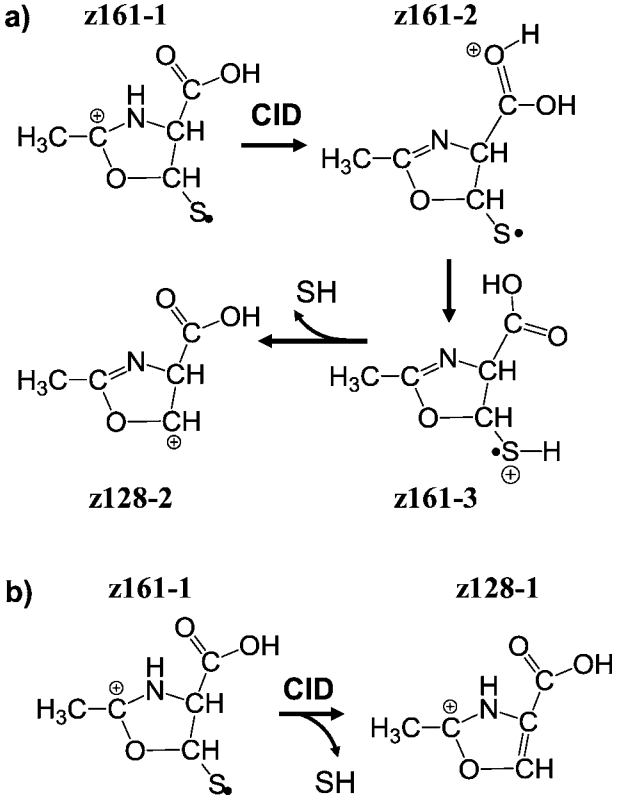

hydrogen to nitrogen to form **z128-1**. However, no stable transition state could be found for this process.

Scheme 3b shows the reaction pathway involving radical-directed hydrogen transfer from C_α (**z161-1**) to the sulfur radical followed by SH loss. The transition state (**TS-5**) contains a four-membered-ring and is 33.1 kcal mol^{-1} higher than **z161-1**. The product ion (**z128-1**) has a five-membered ring with the charge delocalized along the C−N bond of the acetyl group and is a structural isomer of the product formed in the proton-based SH loss (**z128-2**). Comparison of these two isomers shows that **z128-1** has a more planar configuration due to the delocalization of the double bond and charge within the five-membered ring and is 37.0 kcal mol^{-1} more stable than **z128-2**. Isomerization from **z128-2** to **z128-1** requires going through a transition state that is 35.0 kcal mol^{-1} higher in enthalpy than **z128-2**. MS^3 CID of d_3-Ac-$^{SO•}$Cys (Figure 2d) showed that the radical-directed pathway (SD loss) is competitive with the charge-directed fragmentation (SH loss). The kinetic isotope effect may also play a role in the radical-directed DS loss, in which breaking the C−D bond is involved in the rate-limiting step.[55] The relative enthalpies of the key structures for consecutive SH loss from Ac-$^{SO•}$Cys radicals can be found in Table S1 in the Supporting Information, and the spin densities and charge locations are shown in Table S2 in the Supporting Information.

CONCLUSIONS

The gas-phase structures and unimolecular dissociation behavior of intact and modified cysteine sulfinyl radicals were examined using tandem mass spectrometry, stable isotope labeling, and theoretical calculations. Low-energy CID showed that N-acetylation promotes charge-directed H_2O loss and shuts down the radical-directed C_α−C_β bond scission of cysteine sulfinyl radical ions. The theoretical results agreed well with the experimentally observed competition between charge- and radical-directed fragmentation. For the intact protonated $^{SO•}$Cys radicals, the barrier for the radical-directed CH_2SO loss is 26.1 kcal mol^{-1} lower than that of the charge-directed H_2O loss, and the glycyl radical ions formed from CH_2SO loss have a very stable captodative structure. For protonated Ac-$^{SO•}$Cys, the barrier for charge-directed H_2O loss is only 4.2 kcal mol^{-1} higher than that of the CH_2SO loss, thus making this channel competitive. The dominant H_2O loss from Ac-$^{SO•}$Cys could be explained from its favorable kinetics. Facile SH loss was observed after H_2O loss for protonated Ac-$^{SO•}$Cys. This loss can be either charge- or radical-directed. In the charge-directed process, a two-step proton transfer process from nitrogen to sulfur has been invoked, while a four-membered-ring transition state has been

dx.doi.org/10.1021/ja4008744 | J. Am. Chem. Soc. 2013, 135, 6226−6233

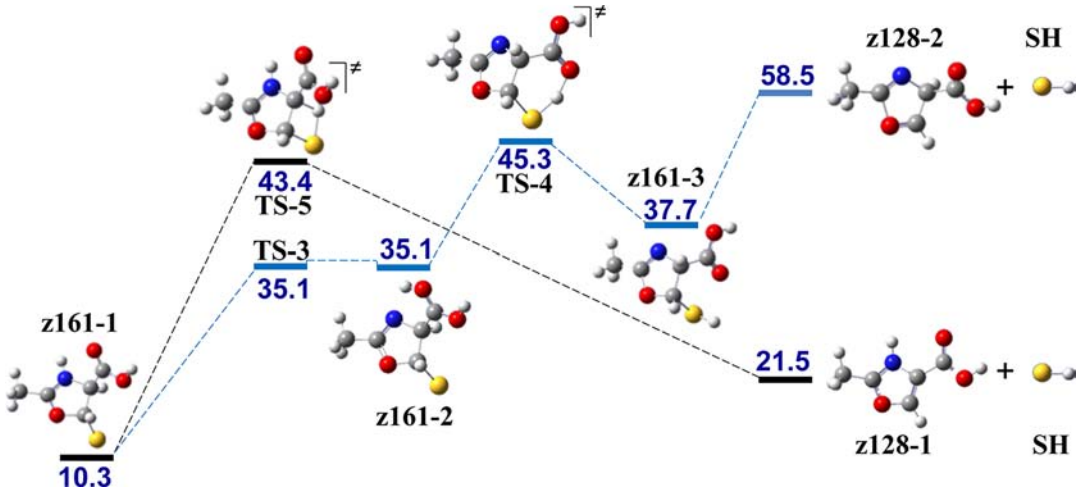

Figure 5. Energetic profile and key structures for consecutive SH loss with competitive proton or hydrogen transfer pathways: (a) charge-directed two-step proton transfer (blue curve); (b) radical-directed C_α hydrogen transfer (black curve). The enthalpies are shown in kcal mol^{-1} and are relative to **Ac-$^{SO\bullet}$Cys-1**.

proposed for radical-directed hydrogen transfer from C_α to sulfur. The potential energy surfaces for these two pathways showed similar energy requirements, which could explain why both channels were observed in CID experiments. Cysteine sulfinyl radical ions present a simple but interesting model for studying the competition between radical- and charge-directed fragmentation. Our results show that the radical-directed C_α–C_β scission is very sensitive to the stability of the glycyl radical ions formed, which affects its competitiveness with charge-directed H_2O loss. The role of acetylation in affecting the competition does not rely heavily on changing the proton affinity of various sites within cysteine sulfinyl radical ions but rather involves modulation of the stability of the product ions. What we learned from cysteine sulfinyl radical ions could also be applied to understanding the fragmentation behavior of hydrogen-deficient peptide radical ions, where C_α–C_β scission has frequently been observed by a radical located at the C_γ position.[31]

■ ASSOCIATED CONTENT

Supporting Information

MS^1 positive nanoESI spectra before and after AP ion/radical reactions of cystine and *N*-acetylcystine (Figure S1); MS^2 or MS^3 ion trap CID spectra of $^{SO\bullet}$Cys-OMe, Ac-$^{SO\bullet}$Cys-OMe, d_2-$^{SO\bullet}$Cys, $^{SO\bullet}$Cys, d_5-Ac-$^{SO\bullet}$Cys, and $^{18}O_2$-Ac-$^{SO\bullet}$Cys (Figures S2–S6); one-step proton transfer for consecutive SH loss (Figure S7); and electronic energies (kcal mol^{-1}), absolute energies (Hartrees), spin densities, atomic charges, and Cartesian coordinates of optimized structures (Tables S1–S4). This material is available free of charge via the Internet at http://pubs.acs.org.

■ AUTHOR INFORMATION

Corresponding Author

francisc@purdue.edu; yxia@purdue.edu

Notes

The authors declare no competing financial interest.

■ ACKNOWLEDGMENTS

The authors acknowledge the Purdue Research Fund and NSF CHE-1248613 for financial support. We acknowledge the Midwest Crossroads Alliance for Graduate Education and the Professoriate (AGEP) Program of Purdue University, which provides research funds for faculty who advise underrepresented students. The authors thank Professor R. G. Cooks for the use of the LTQ Orbitrap instrument.

■ REFERENCES

(1) Stubbe, J.; van der Donk, W. A. *Chem. Rev.* **1998**, *98*, 705–762.
(2) Segal, A. W. *Annu. Rev. Immunol.* **2005**, *23*, 197–223.
(3) Nathan, C. *Nature* **2003**, *422*, 675–676.
(4) Berlett, B. S.; Stadtman, E. R. *J. Biol. Chem.* **1997**, *272*, 20313–20316.
(5) Halliwell, B.; Gutteridge, J. M. C. *Free Radicals in Biology and Medicine*, 4th ed.; Oxford University Press: New York, 2007
(6) Tureček, F.; Carpenter, F. H.; Polce, M. J.; Wesdemiotis, C. *J. Am. Chem. Soc.* **1999**, *121*, 7955–7956.
(7) Hopkinson, A. C. *Mass Spectrom. Rev.* **2009**, *28*, 655–671.
(8) Ryzhov, V.; Lam, A. K. Y.; O'Hair, R. A. J. *J. Am. Soc. Mass Spectrom.* **2009**, *20*, 985–995.
(9) Chu, I. K.; Laskin, J. *Eur. J. Mass Spectrom.* **2011**, *17*, 543–556.
(10) Hodyss, R.; Cox, H. A.; Beauchamp, J. L. *J. Am. Chem. Soc.* **2005**, *127*, 12436–12437.
(11) Masterson, D. S.; Yin, H.; Chacon, A.; Hachey, D. L.; Norris, J. L.; Porter, N. A. *J. Am. Chem. Soc.* **2004**, *126*, 720–721.
(12) Wee, S.; Mortimer, A.; Moran, D.; Wright, A.; Barlow, C. K.; O'Hair, R. A. J.; Radom, L.; Easton, C. J. *Chem. Commun.* **2006**, 4233–4235.
(13) Parthasarathi, R.; He, Y.; Reilly, J. P.; Raghavachari, K. *J. Am. Chem. Soc.* **2010**, *132*, 1606–1610.
(14) Ly, T.; Julian, R. R. *Angew. Chem., Int. Ed.* **2009**, *48*, 7130–7137.
(15) Moore, B. N.; Ly, T.; Julian, R. R. *J. Am. Chem. Soc.* **2011**, *133*, 6997–7006.
(16) Barlow, C. K.; Wright, A.; Easton, C. J.; O'Hair, R. A. J. *Org. Biomol. Chem.* **2011**, *9*, 3733–3745.
(17) Moore, B. N.; Blanksby, S. J.; Julian, R. R. *Chem. Commun.* **2009**, 5015–5017.
(18) Sinha, R. K.; Maitre, P.; Piccirillo, S.; Chiavarino, B.; Crestoni, M. E.; Fornarini, S. *Phys. Chem. Chem. Phys.* **2010**, *12*, 9794–9800.
(19) Osburn, S.; Berden, G.; Oomens, J.; O'Hair, R.; Ryzhov, V. *J. Am. Soc. Mass Spectrom.* **2011**, *22*, 1794–1803.
(20) McLafferty, F. W.; Tureček, F. *Interpretation of Mass Spectra*, 4th ed.; University Science Books: Sausalito, CA, 1993.
(21) Viehe, H. G.; Janousek, Z.; Merenyi, R.; Stella, L. *Acc. Chem. Res.* **1985**, *18*, 148–154.
(22) Sack, T. M.; Cerny, R. L.; Gross, M. L. *J. Am. Chem. Soc.* **1985**, *107*, 4562–4564.

(23) Yates, B. F.; Bouma, W. J.; Radom, L. *Tetrahedron* **1986**, *42*, 6225−6234.
(24) Stirk, K. M.; Kiminkinen, L. K. M.; Kenttamaa, H. I. *Chem. Rev.* **1992**, *92*, 1649−1665.
(25) Ly, T.; Julian, R. R. *J. Am. Soc. Mass Spectrom.* **2009**, *20*, 1148−1158.
(26) Osburn, S.; Steill, J. D.; Oomens, J.; O'Hair, R. A. J.; van Stipdonk, M.; Ryzhov, V. *Chem.—Eur. J.* **2011**, *17*, 873−879.
(27) Steill, J.; Zhao, J. F.; Siu, C. K.; Ke, Y. Y.; Verkerk, U. H.; Oomens, J.; Dunbar, R. C.; Hopkinson, A. C.; Siu, K. W. M. *Angew. Chem., Int. Ed.* **2008**, *47*, 9666−9668.
(28) Barlow, C. K.; Moran, D.; Radom, L.; McFadyen, W. D.; O'Hair, R. A. J. *J. Phys. Chem. A* **2006**, *110*, 8304−8315.
(29) Siu, C. K.; Ke, Y.; Guo, Y.; Hopkinson, A. C.; Siu, K. W. M. *Phys. Chem. Chem. Phys.* **2008**, *10*, 5908−5918.
(30) Zhao, J. F.; Ng, C. M. D.; Chu, I. K.; Siu, K. W. M.; Hopkinson, A. C. *Phys. Chem. Chem. Phys.* **2009**, *11*, 7629−7639.
(31) Sun, Q.; Nelson, H.; Ly, T.; Stoltz, B. M.; Julian, R. R. *J. Proteome Res.* **2009**, *8*, 958−966.
(32) Siu, C. K.; Ke, Y. Y.; Orlova, G.; Hopkinson, A. C.; Siu, K. W. M. *J. Am. Soc. Mass Spectrom.* **2008**, *19*, 1799−1807.
(33) Zhang, L. Y.; Reilly, J. P. *J. Am. Soc. Mass Spectrom.* **2009**, *20*, 1378−1390.
(34) Laskin, J.; Yang, Z. B.; Ng, C. M. D.; Chu, I. K. *J. Am. Soc. Mass Spectrom.* **2010**, *21*, 511−521.
(35) Dongré, A. R.; Jones, J. L.; Somogyi, Á.; Wysocki, V. H. *J. Am. Chem. Soc.* **1996**, *118*, 8365−8374.
(36) Kalli, A.; Hess, S. *J. Am. Soc. Mass Spectrom.* **2012**, *23*, 244−263.
(37) Tan, L.; Xia, Y. *J. Am. Soc. Mass Spectrom.* **2012**, *23*, 2011−2019.
(38) Ma, X.; Love, C.; Zhang, X.; Xia, Y. *J. Am. Soc. Mass Spectrom.* **2011**, *22*, 922−930.
(39) Wee, S.; O'Hair, R. A. J.; McFadyen, W. D. *Int. J. Mass Spectrom.* **2006**, *249*, 171−183.
(40) Tao, Y.; Quebbemann, N. R.; Julian, R. R. *Anal. Chem.* **2012**, *84*, 6814−6820.
(41) Xu, M. J.; Song, T.; Quan, Q. A.; Hao, Q. A.; Fang, D. C.; Siu, C. K.; Chu, I. K. *Phys. Chem. Chem. Phys.* **2011**, *13*, 5888−5896.
(42) Lam, A. K. Y.; Ryzhov, V.; O'Hair, R. A. J. *J. Am. Soc. Mass Spectrom.* **2010**, *21*, 1296−1312.
(43) Chu, I. K.; Zhao, J.; Xu, M.; Siu, S. O.; Hopkinson, A. C.; Siu, K. W. M. *J. Am. Chem. Soc.* **2008**, *130*, 7862−7872.
(44) Song, T.; Ng, D. C. M.; Quan, Q. A.; Siu, C. K.; Chu, I. K. *Chem.—Asian J.* **2011**, *6*, 888−898.
(45) Zhao, J. F.; Song, T.; Xu, M. J.; Quan, Q.; Siu, K. W. M.; Hopkinson, A. C.; Chu, I. K. *Phys. Chem. Chem. Phys.* **2012**, *14*, 8723−8731.
(46) Xia, Y.; Cooks, R. G. *Anal. Chem.* **2010**, *82*, 2856−2864.
(47) Reddy, S. G.; Wong, K. K.; Parast, C. V.; Peisach, J.; Magliozzo, R. S.; Kozarich, J. W. *Biochemistry* **1998**, *37*, 558−563.
(48) Gauld, J. W.; Eriksson, L. A. *J. Am. Chem. Soc.* **2000**, *122*, 2035−2040.
(49) Sevilla, M. D.; Becker, D.; Swarts, S.; Herrington, J. *Biochem. Biophys. Res. Commun.* **1987**, *144*, 1037−1042.
(50) Frisch, M. J.; Trucks, G. W.; Schlegel, H. B.; Scuseria, G. E.; Robb, M. A.; Cheeseman, J. R.; Scalmani, G.; Barone, V.; Mennucci, B.; Petersson, G. A.; Nakatsuji, H.; Caricato, M.; Li, X.; Hratchian, H. P.; Izmaylov, A. F.; Bloino, J.; Zheng, G.; Sonnenberg, J. L.; Hada, M.; Ehara, M.; Toyota, K.; Fukuda, R.; Hasegawa, J.; Ishida, M.; Nakajima, T.; Honda, Y.; Kitao, O.; Nakai, H.; Vreven, T.; Montgomery, J. A., Jr.; Peralta, J. E.; Ogliaro, F.; Bearpark, M.; Heyd, J. J.; Brothers, E.; Kudin, K. N.; Staroverov, V. N.; Kobayashi, R.; Normand, J.; Raghavachari, K.; Rendell, A.; Burant, J. C.; Iyengar, S. S.; Tomasi, J.; Cossi, M.; Rega, N.; Millam, J. M.; Klene, M.; Knox, J. E.; Cross, J. B.; Bakken, V.; Adamo, C.; Jaramillo, J.; Gomperts, R.; Stratmann, R. E.; Yazyev, O.; Austin, A. J.; Cammi, R.; Pomelli, C.; Ochterski, J. W.; Martin, R. L.; Morokuma, K.; Zakrzewski, V. G.; Voth, G. A.; Salvador, P.; Dannenberg, J. J.; Dapprich, S.; Daniels, A. D.; Farkas, Ö.; Foresman, J. B.; Ortiz, J. V.; Cioslowski, J.; Fox, D. J. *Gaussian 09*, revision A.1; Gaussian, Inc.: Wallingford, CT, 2009.
(51) Becke, A. D. *J. Chem. Phys.* **1993**, *98*, 5648−5652.
(52) Lee, C.; Yang, W.; Parr, R. G. *Phys. Rev. B* **1988**, *37*, 785−789.
(53) Gonzalez, C.; Schlegel, H. B. *J. Chem. Phys.* **1989**, *90*, 2154−2161.
(54) Bartlett, R. J. *Annu. Rev. Phys. Chem.* **1981**, *32*, 359−401.
(55) Wiberg, K. B. *Chem. Rev.* **1955**, *55*, 713−743.